The State Scientific Center of Russia

The Budker Institute of Nuclear Physics
SB RAS

V.M.Aulchenko, M.N.Achasov, T.V.Baier,
P.M.Beschastnov, A.D.Bukin, D.A.Bukin,
S.V.Burdin, A.V.Bozhenok, B.O.Baibusinov,
V.V.Danilov, S.I.Dolinsky, V.P.Druzhinin,
M.S.Dubrovin, I.A.Gaponenko, V.B.Golubev,
V.N.Ivanchenko, S.V.Koshuba, A.A.Korol,
I.A.Koop, A.P.Lysenko, I.N.Nesterenko,
E.V.Pakhtusova, E.A.Perevedentsev, A.A.Polunin,
V.I.Ptitsyn, E.G.Pozdeev, A.A.Salnikov,
S.I.Serednyakov, Yu.M.Shatunov, M.A.Shubin,
V.A.Sidorov, Z.K.Silagadze, A.N.Skrinsky,
Yu.V.Usov, Yu.S.Velikzhanin

BEGINNING OF THE EXPERIMENTS WITH SND DETECTOR AT e^+e^- COLLIDER VEPP-2M

Budker INP 95-56

НОВОСИБИРСК

Beginning of the Experiments with SND Detector at e^+e^- Collider VEPP-2M[1]

V.M.Aulchenko, M.N.Achasov, T.V.Baier, P.M.Beschastnov, A.D.Bukin, D.A.Bukin, S.V.Burdin, A.V.Bozhenok, B.O.Baibusinov, V.V.Danilov, S.I.Dolinsky, V.P.Druzhinin, M.S.Dubrovin, I.A.Gaponenko, V.B.Golubev, V.N.Ivanchenko, S.V.Koshuba, A.A.Korol, I.A.Koop, A.P.Lysenko, I.N.Nesterenko, E.V.Pakhtusova, E.A.Perevedentsev, A.A.Polunin, V.I.Ptitsyn, E.G.Pozdeev, A.A.Salnikov, S.I.Serednyakov, Yu.M.Shatunov, M.A.Shubin, V.A.Sidorov, Z.K.Silagadze, A.N.Skrinsky, Yu.V.Usov, Yu.S.Velikzhanin

The Budker Institute of Nuclear Physics,
630090, Novosibirsk, Russia

Abstract

Experiments have been started with nonmagnetic SND detector at the VEPP-2M collider to study e^+e^- annihilation in a 1 GeV center of mass energy region. The main part of the SND is a three layer spherical NaI(Tl) calorimeter, consisted of 1632 individual crystals. The calorimeter thickness is 13.5 radiation lengths and its total mass is 3.6 tons. Inner part of the detector is a cylindrical drift chamber system for charge particles tracking. Outside the calorimeter the muon/veto detector is installed, which consists of streamer tubes and scintillation counters. The preliminary results on some SND parameters, obtained from the test run at VEPP-2M collider, are presented.

[1]Submitted to HADRON–95 Conference, Manchester, July 10–14, 1995

1 VEPP-2M collider

Electron-positron collider VEPP-2M is the world only e^+e^- machine in a pre-ϕ-factory era, operating in the energy range 2E from 0.4 to 1.4 GeV, covering the energies of resonance production of lightest quarkonia: ρ, ω, ϕ. Collider complex VEPP-2M (Fig. 1) consists of an injector part with 3 MeV linear accelerator ILU and 200 MeV electron synchrobetatron B-3M, 900 MeV booster synchrotron BEP for accumulation of electrons and positrons, and 700 MeV collider VEPP-2M [1]. The maximum luminosity of VEPP-2M depends on its energy in accordance with E^4 law, and at the energy of 2E = 1000 MeV it is equal to $3 \cdot 10^{30} \mathrm{cm}^{-2}\mathrm{sec}^{-1}$. The previous longest experimental run at VEPP-2M was performed with a Neutral Detector (ND) [2]. The physical results obtained with ND, were based on integrated luminosity of 19 inverse picobarns [3]. In 1992 experiments with CMD-2 detector [4] started, and in early 1995 a new nonmagnetic Spherical Neutral Detector (SND) [5] began data acquisition as well. Now both CMD-2 and SND detectors, located in opposite straight sections of VEPP-2M, take data in parallel.

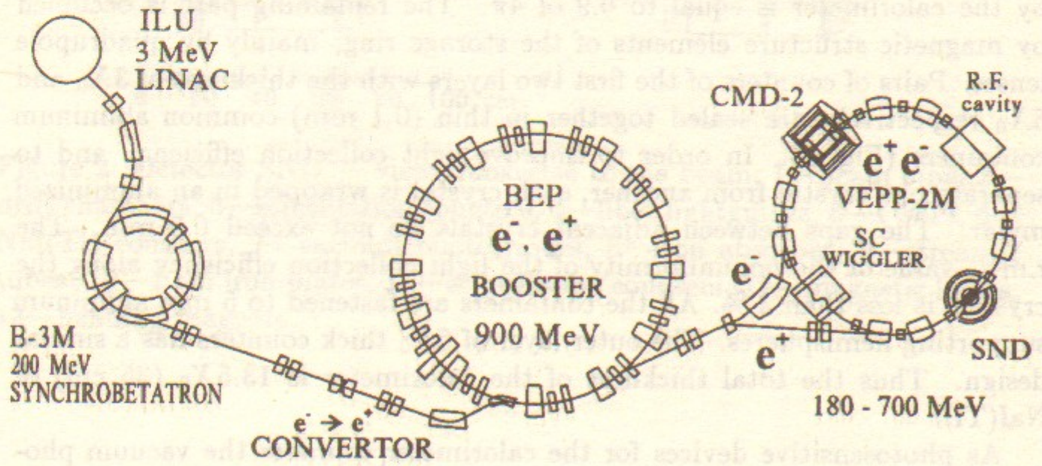

Figure 1: Layout of VEPP-2M collider complex

2 SND detector

2.1 Detector overview

The main part of SND (Fig. 2,3) is a 3-layer spherical NaI(Tl) electromagnetic calorimeter. Tracking system, located in the detector center, consists of two coaxial cylindrical drift chambers. In the radial gap between them a 5 mm thick plastic scintillation counter with wavelength shifter fiber readout is installed. From outside the calorimeter is covered by a thick (12 cm) iron absorber, which attenuates residuals of electromagnetic showers. An outer muon/veto system is located outside the absorber. It consists of sheets of plastic scintillator and streamer tubes.

2.2 Calorimeter

Each calorimeter layer is divided into separate counters in the following way (Fig. 4): in the azimuthal direction it is divided into 40 equal parts by planes with 9° angle between adjacent ones. Each part is further divided in polar direction into pieces with equal angles $\Delta\vartheta = 9°$. Crystals at polar angles less than 36° or greater than 144° are 18° in azimuthal direction. The closest to the beam crystals of the inner layer, corresponding to polar angles less than 27° or greater than 153°, were removed. Each layer of the calorimeter includes 520–560 crystals of eight different shapes. Most of the crystals have shapes of truncated tetrahedral pyramids. The total solid angle covered by the calorimeter is equal to 0.9 of 4π. The remaining part is occupied by magnetic structure elements of the storage ring, mainly by quadrupole lenses. Pairs of counters of the first two layers with the thickness of $3X_0$ and $5X_0$ respectively are sealed together in thin (0.1 mm) common aluminum containers (Fig. 5). In order to improve light collection efficiency and to separate one crystal from another, each crystal is wrapped in an aluminized mylar. The gaps between adjacent crystals do not exceed 0.5 mm. The r.m.s. value of the nonuniformity of the light collection efficiency along the crystals is less than 3 %. All the containers are fastened to 5 mm aluminum supporting hemispheres. The outer layer of $6X_0$ thick counters has a similar design. Thus the total thickness of the calorimeter is $13.5X_0$ (35 cm) of NaI(Tl).

As photosensitive devices for the calorimeter counters the vacuum phototriodes are used. The quantum efficiency of their photocathodes is about 15 %, average gain is 10 and light collection efficiency is about 10 %. Signals from phototriodes are amplified by charge sensitive preamplifiers located di-

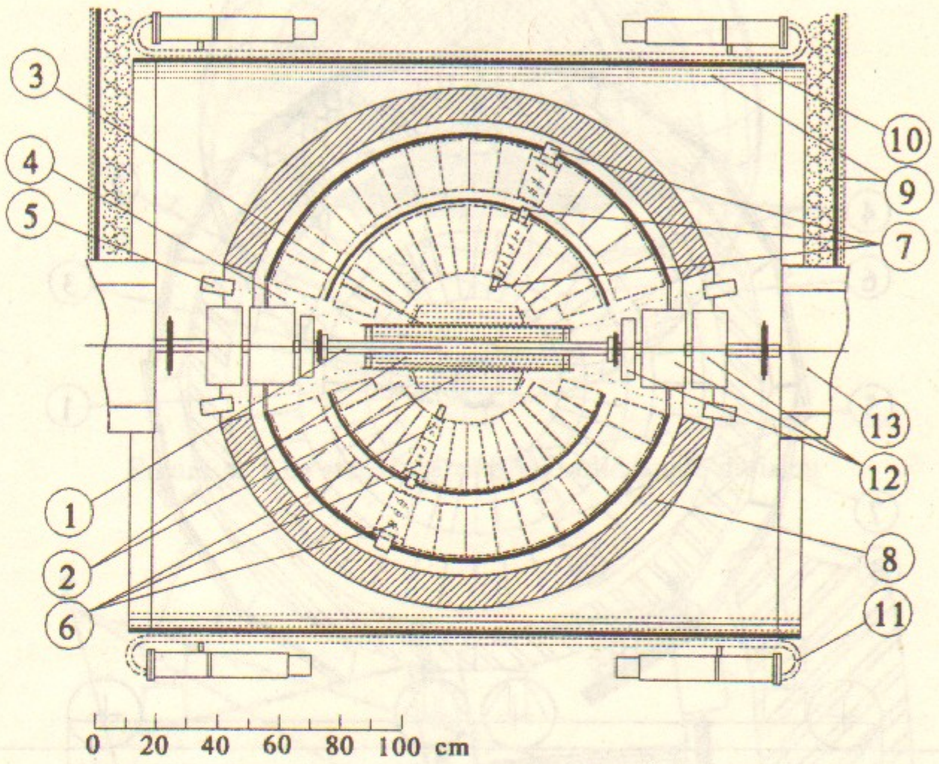

Figure 2: Detector SND — view transverse to the beam; 1—beam pipe, 2—drift chambers, 3—scintillation counters, 4—fiber lightguides, 5—PMTs, 6—NaI(Tl) counters, 7—vacuum phototriodes, 8—iron absorber, 9—streamer tubes, 10—1 cm iron plates, 11—scintillation counters, 12—magnetic lenses, 13—bending magnets

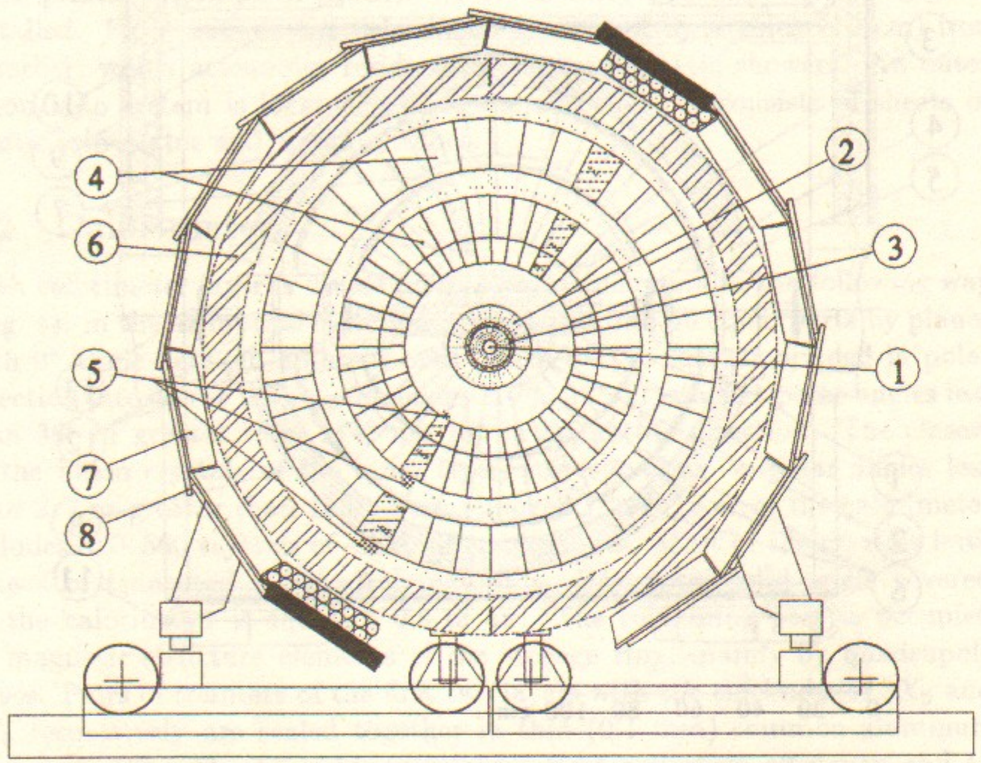

Figure 3: Detector SND — view along the beam; 1—beam pipe, 2—drift chambers, 3—scintillation counters; 4—NaI(Tl) counters, 5—phototriodes, 6—iron absorber, 7—streamer tubes, 8—scintillation counters

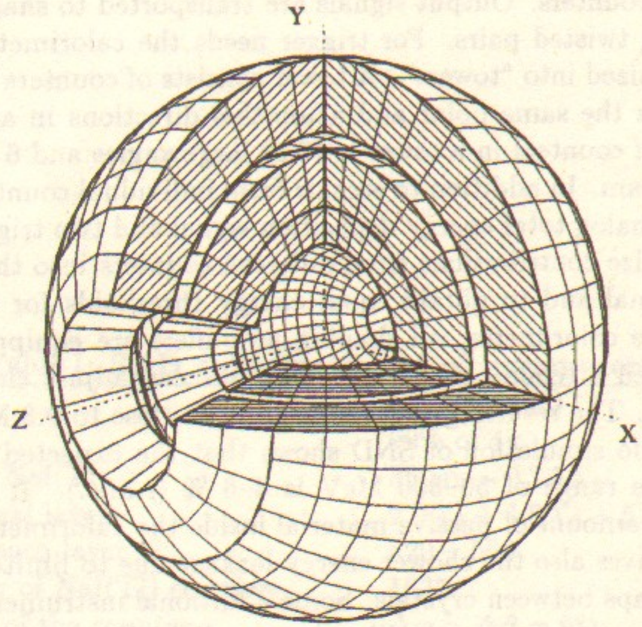

Figure 4: The structure of SND solid angle division

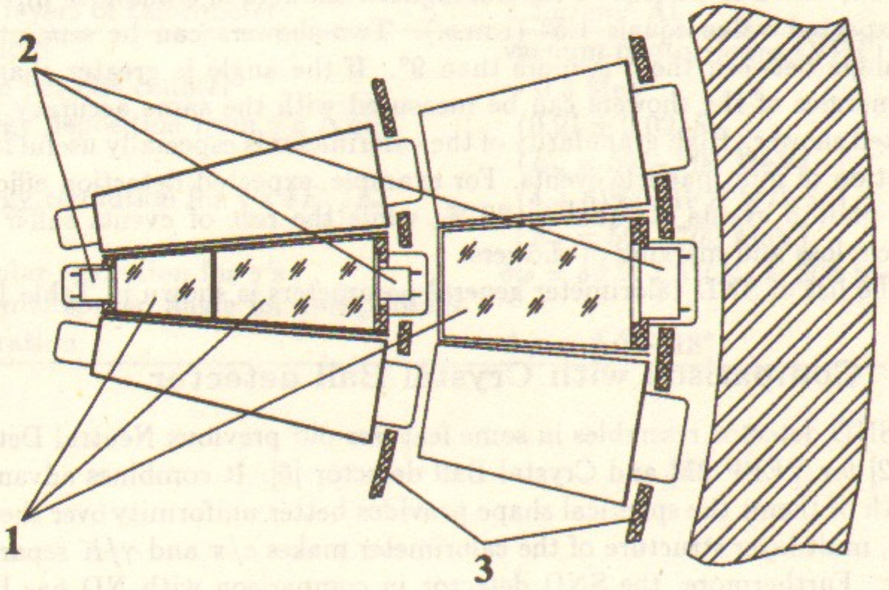

Figure 5: The view of NaI(Tl) crystals in calorimeter, 1—NaI(Tl) crystals, 2—vacuum phototriodes, 3—aluminum supporting hemispheres

rectly on the counters. Output signals are transported to shaping amplifiers via 20 m long twisted pairs. For trigger needs the calorimeter crystals are logically organized into "towers". A tower consists of counters located within 18° interval in the same polar and azimuthal directions in all three layers. The number of counters in a tower is 12 at large angles and 6 in the regions, close to the beam. In addition to signals from individual counters each tower produces an analog total energy deposition signal and two trigger signals. In order to equalize contributions from different counters into the total energy deposition signal and to obtain equal energy thresholds for trigger signals over the whole calorimeter, all shaping amplifiers are equipped with computer controlled attenuators, using which, one can adjust channels gain in steps of 1/255. The resulting electronics noise is close to 0.3 MeV (r.m.s.).

Monte Carlo simulation of SND shows that the expected resolution for photons in the range of 50–500 MeV is 4–6 % (r.m.s.). It is determined mostly by the amount of passive material inside the calorimeter. Noticeable contribution gives also the shower energy leakage due to limited thickness of NaI(Tl) and gaps between crystals. Some additional instrumentation factors like electronics noise, errors in calibration, nonlinearity and instability of the electronics also contribute into total energy resolution of the calorimeter.

The angular resolution of the calorimeter is determined by the size of its elements and fluctuations of electromagnetic showers in transverse direction. Its expected value equals 1.5° (r.m.s.). Two showers can be separated, if the angle between them is more than 9°. If the angle is greater than 18°, the energies of the showers can be measured with the same accuracy as for isolated shower. High granularity of the calorimeter is especially useful for the detection of multiparticle events. For example, expected detection efficiency for 6-photon events is equal to 60 %, while the rest of events suffer from particle loss and merging of showers.

The list of SND calorimeter general parameters is shown in Table 1.

2.3 Comparison with Crystal Ball detector

The SND detector resembles in some features our previous Neutral Detector ND [2] for VEPP-2M and Crystal Ball detector [6]. It combines advantages of both of them: the spherical shape provides better uniformity over the solid angle; multilayer structure of the calorimeter makes e/π and γ/K separation easier. Furthermore, the SND detector in comparison with ND has better energy and angular resolution and much better hermeticity.

Table 1: **SND calorimeter list of parameters**

Total weight	3.5 t NaI(Tl)
Solid angle	90% of 4π
Thickness of NaI(Tl)	35 cm $\sim 13.5X_0$
Three spherical layers	$2.9X_0 + 4.8X_0 + 5.8X_0$
Counters in each layer	520 – 560
Total number of NaI(Tl) counters	1632
Angular size of the counter	$\Delta\varphi = \Delta\vartheta = 9°$
Amount of material between the drift chamber and calorimeter	2.3 g/cm^2 Al
Amount of material between 2-nd and 3-rd layers of calorimeter	2.2 g/cm^2 Al
Readout	vacuum phototriodes (VPT)
Noise per one counter	$\sim$ 0.3 MeV
Energy deposition from γ's ΔE_γ	$(0.91 \pm 0.02)E_0$ ($E_\gamma = 50 - 700$ MeV)
Energy resolution for γ's $\delta E_\gamma / E_\gamma$	$(4 \div 6)\%(FWHM/2.36)$ ($E_\gamma = 50 - 700$ MeV)
Angular resolution for γ's	$\delta\varphi = \delta\vartheta = 1.5°(E_\gamma = 300$ MeV)
Minimal spatial angle for two photons separation	$\Delta\varphi \sim \Delta\vartheta \sim 18°$

2.4 Tracking system

Tracking system consists of two cylindrical drift chambers (Fig. 6). The length of the chamber closest to the beam is 40 cm, its inner and outer diameters are 4 and 12 cm respectively. The corresponding dimensions of the outer chamber are 25, 14 and 24 cm. Both chambers are divided into 20 jet-type cells in azimuthal plane. Each cell contains 5 sensitive wires. Longitudinal coordinate is measured by charge division method with the accuracy of 3 mm. In addition, cathode strips readout for inner and outer layers provides the improvement of the latter value to 0.5 mm. Outer drift chamber improves pattern recognition for multiparticle events. The overall angular resolution of the drift chamber system is 0.3 – 0.4° in azimuthal and polar direction respectively. The impact parameter resolution is 0.5 mm. The solid angle for inner chamber is 96 % of 4π. The parameters of drift chamber system are listed in Table 2.

2.5 Muon detector

SND muon/veto system consists of plastic scintillation counters and streamer tubes [11]. It is intended mainly for cosmic background suppression for the events without charged particles. The probability of its triggering by the events of the reaction $e^+e^- \to \gamma\gamma$ at the maximum available energy is less then 1 %. Muons of the reaction $e^+e^- \to \mu^+\mu^-$, starting from the beam energy about 500 MeV, go out from the absorber and trigger the muon detector. The muon/veto system is not included as a component in a charged particle trigger.

2.6 Trigger

The three level trigger of the detector selects events of different types: events with photons only, events with charged particles, and cosmic muon events for detector calibration. The drift chamber first level trigger (FLT) searches for tracks in the drift chambers with the impact parameter $\Delta r < 20$ mm. The calorimeter FLT uses total energy deposition in the calorimeter and double coincidences of calorimeter towers with a threshold of 30 MeV.

The second level trigger processor (SLT), which is not fully implemented yet, will select tracks with $\Delta r < 2$ mm and isolated clusters in the calorimeter, which look like individual showers.

The third level trigger (TLT), which is implemented now as a special fast computer code on a main data acquisition computer, checks events be-

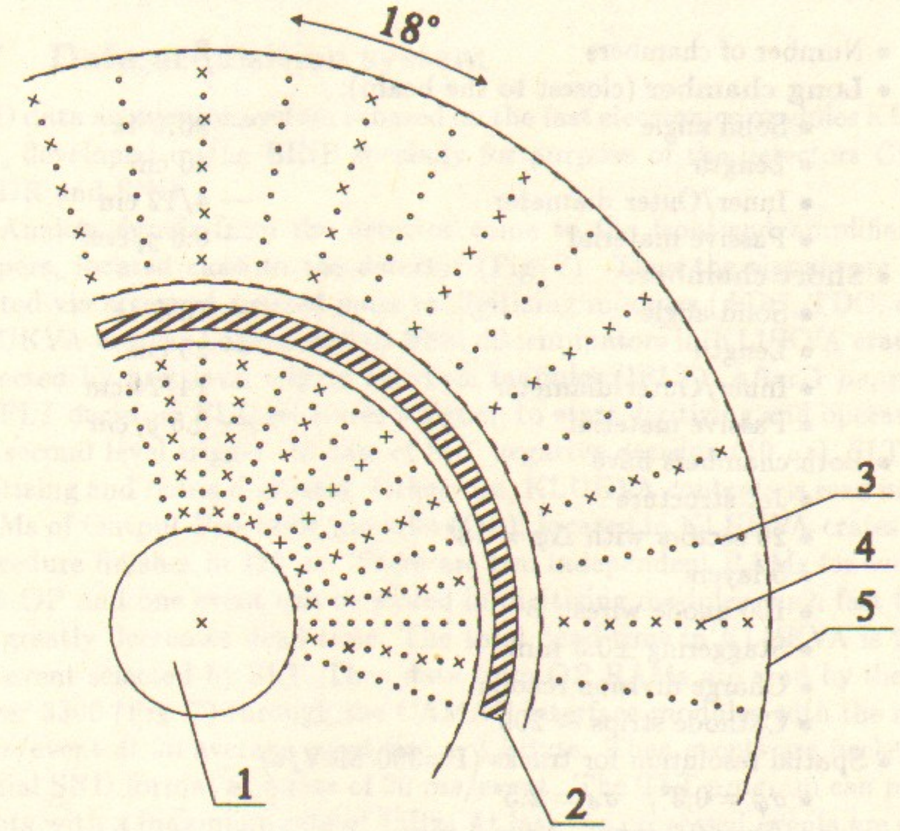

Figure 6: The layout of SND drift chambers, 1—beam pipe, 2—plastic scintillation counters, 3—field wires, 4—sense wires, 5—field shaping strips

Table 2: **List of SND drift chamber system parameters**

- Number of chambers — 2
- **Long chamber** (closest to the beam):
  - Solid angle — 96% 4π
  - Length — 40 cm
  - Inner/Outer diameter — 4/12 cm
  - Passive material — 0.3 g/cm^2
- **Short chamber:**
  - Solid angle — 70% 4π
  - Length — 25 cm
  - Inner/Outer diameter — 14/24 cm
  - Passive material — 0.5 g/cm^2
- Both chambers have
  - Jet structure
  - 20 sectors with $\Delta\varphi = 18°$
  - 5 layers
  - 100 anode wires
  - Staggering ± 0.3 mm
  - Charge division readout
  - Cathode strips $\sim$ 200
- Spatial resolution for tracks (P=300 MeV/c)
  - $\sigma_\varphi = 0.3°$, $\sigma_\vartheta = 2.5°$
  - $\Delta r = 0.3$ mm, $\Delta z = 3$ mm
- Plastic scintillator between chambers:
  - $0.9 g/cm^2$
- Beam pipe: $0.15 g/cm^2$

fore recording them on tape, rejects cosmics events with charged trigger, and suppresses beam background using z-coordinates of tracks, measured by drift chambers. In addition TLT identifies collinear events of Bhabha scattering and 2-γ annihilation. These events are used for monitoring collider luminosity. In future it is planned to use TLT for identification of events of main resonant reactions, and to write on tape only a small fraction of the identified events.

2.7 Data acquisition system

SND data acquisition system is based on the fast electronics modules KLUKVA [12], developed in the BINP specially for purpose of the detectors CMD-2, KEDR and SND.

Analog signals from the detector come to the front-end amplifiers and shapers, located close to the detector (Fig. 7). Then the signals are transmitted via screened twisted pairs to digitizing modules (ADC, TDC, etc) in KLUKVA crates. Logical signals from discriminators in KLUKVA crates are collected by first level trigger interface modules (IFLT). After 1 μs, needed for FLT decision, FLT generates a signal, to start digitizing and operation of the second level trigger. In case of SLT negative decision (10 μs), SLT stops digitizing and resets digitizers. Otherwise, KLUKVA contents is read into the RAMs of Output Processor modules (OP), located in KLUKVA crates. This procedure finishes in 120 μs. There are two independent RAMs for events in each OP and one event can be stored in digitizing modules, such fast buffering greatly decreases dead time. The total dead time in KLUKVA is 200 μs per event selected by SLT. Then data from OP RAMs are read by the VAX server 3300 (Fig. 7) through the CAMAC interface modules with the rate of 2 ms/event at an average event size $\sim$ 1 kByte. Then events are packed in a special SND format at a rate of 20 ms/event. The TLT program can process events with a maximum rate of 45Hz. At last the processed events are stored on 8 mm 5 GByte EXABYTE tape.

3 First data taking run at VEPP-2M

In the beginning of 1995 all SND systems have been successfully tested. The background trigger rate from cosmic rays and the beam was found to be not too high. That time SND started operation in parallel with CMD-2 detector. The VEPP-2M initial energy 2E was near 800 MeV, and the average luminosity without wiggler magnet was about $2 \cdot 10^{29} \mathrm{cm}^{-2}\mathrm{sec}^{-1}$.

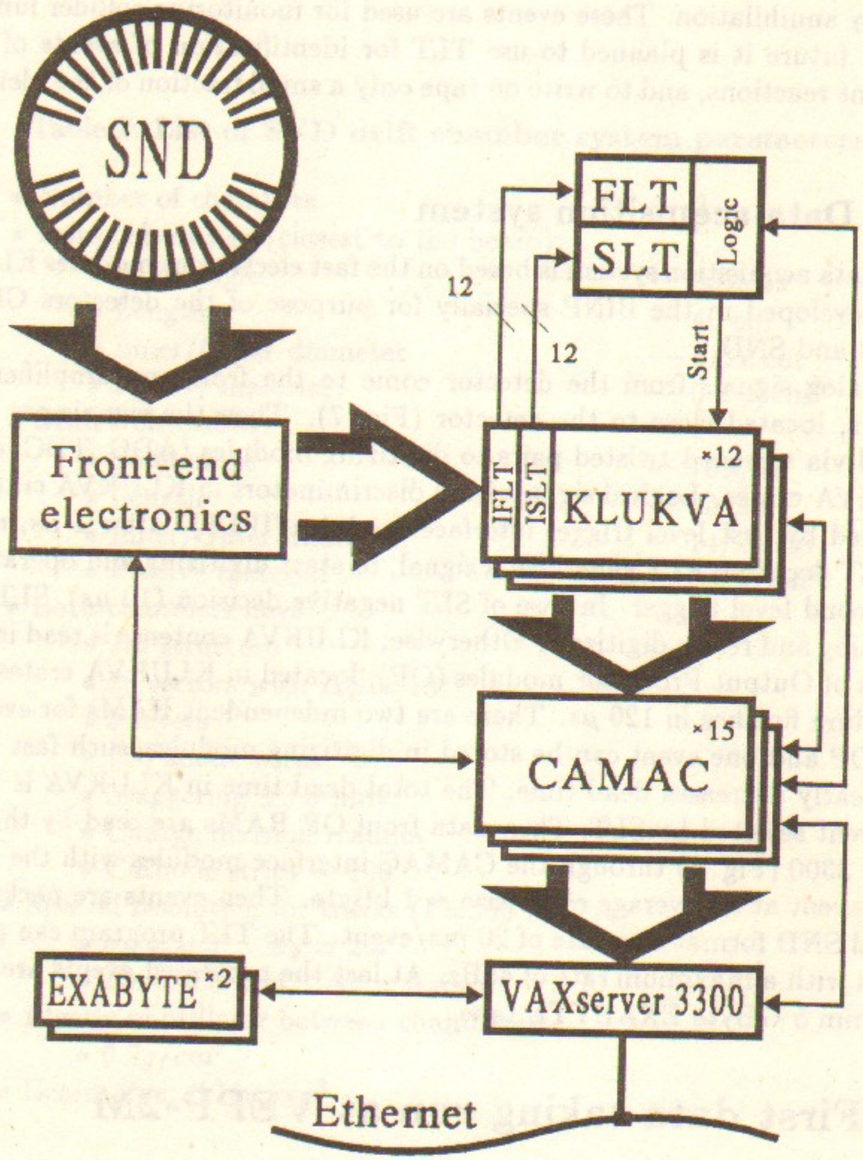

Figure 7: SND data acquisition system

The goal of the SND test run was to adjust trigger components and calibrate main detector systems — calorimeter and drift chambers. Four FLT event patterns have been set during this run: FLT1 — one charged particle and one photon at large angle; FLT2 — two collinear charged particles; FLT3 — two photons at large angle; FLT4 — two collinear photons. An additional FLT5 trigger was used for calorimeter calibration with cosmic rays. In triggers with no charged particles (FLT3, FLT4) signals from the outer system (drift tubes and scintillator counter) and inner drift chamber system have been included in anticoincidence. The total energy deposition threshold about 200 MeV was also included into each trigger pattern. The total trigger rate with two beams in collider was 10–20 Hz and the dead time was 10-20%. The TLT selection program on VAX data acquisition computer reduced the number of recorded events by about a factor of two. The number of recorded events per integrated luminosity was about 10^5events × nb. The average event length on tape was about 0.5 kByte, the events were recorded in files of maximum 25,000 events. In addition to events, on the same tape were recorded: ADC pedestals, ADC and TDC data from pulse generator, scalers, information from VEPP-2M (NMR frequency, beam current etc.), summary of detector performance during current run, etc.

4 The problem of the calorimeter calibration

Now there are two methods in use for absolute energy calibration of the calorimeter: 1 — cosmic rays calibration and 2 — calibration, based on Bhabha scattering events.

1. For cosmic rays calibration events were selected by trigger, containing a track in calorimeter, with at least two fired calorimeter towers with total energy deposition of more than 50 MeV. Then, events were selected by special program in VAX3300 computer, where cosmic muon crossed at least one crystal approximately perpendicular to one of its planes. For each crystal amplitude spectra, normalized for track length in crystal, were stored and then compared with simulated ones.

To calibrate SND calorimeter one day is needed to store about 1000 events per crystal, which allows to reach statistical accuracy of about 1%. Calibration of this type is done once a month. More frequently, during each shift, ADCs are calibrated using pulse generator. For that, pulses from generator are put on preamps input through calibration capacitor. The idea of the algorithm used in SND calibration procedure is the following:

E(MeV)/U(ADC chan.) = E(MeV)/U(gener. code)×
×U(gener. code)/U(ADC chan.)

where E(MeV)/U(gener.code) ratio is obtained during seldom cosmic calibration runs, while the values of U(gener.code)/U(ADC chan.) is measured each shift and in case of replacement of electronics modules. Full calibration algorithm takes into account also nonlinearity of ADCs and generator pedestal. The dependence of ADC code on input amplitude is considered to be described by 2-nd order polynome determined by three coefficients. To obtain all these coefficients, ADC calibration is done with two different settings of programmable attenuators, integrated with shapers, and with a set of different generator amplitudes.

2. Another way of absolute calibration of the crystals of SND calorimeter is to use Bhabha scattering events. Average amplitudes in each crystal for experimental Bhabha events and those for Monte Carlo events were used to obtain the normalizing factors. When the simulated average amplitudes are calculated, the symmetry of the detector is taken into account, that gives the essential improvement of statistical accuracy. Because of strong non–uniformity of the events distribution over ϑ–angle, rather high integrated luminosity is necessary for the accurate calibration of crystals in the $\vartheta \sim 90°$ direction. For example, at the energy of $2E = 800$ MeV the integrated luminosity $L \approx 25$ nb^{-1} is needed to achieve statistical accuracy not worse than 5 % in calibration coefficients for all crystals.

The quality of calibration can be checked with the same Bhabha events. Fig. 8 shows the distribution over normalized energy deposition for collinear charged particles at the energy of $2E = 800$ MeV. The plot corresponds to the integrated luminosity $L \approx 1.5$ nb^{-1}. For calibration in Fig. 8 there were used the events of cosmic ray and $e^+e^- \to e^+e^-, \gamma\gamma$. Measured resolution (Fig. 8) is about two times worse than expected. The origin of disagreement is under study now.

Fig. 9 shows measured and simulated two photon effective mass spectra. A clear π^0–peak is visible in both distributions.

5 Measured parameters of drift chambers

During the experimental run the drift chambers operated with a gas mixture Ar + 10% CO_2. Measurements with Bhabha scattering events showed, that each layer of the chambers had efficiency not worse than 99%. Spatial resolution in each layer is about 0.2 mm in $r - \varphi$ plane. Corresponding deviation in the direction along the wires, measured by charge division method,

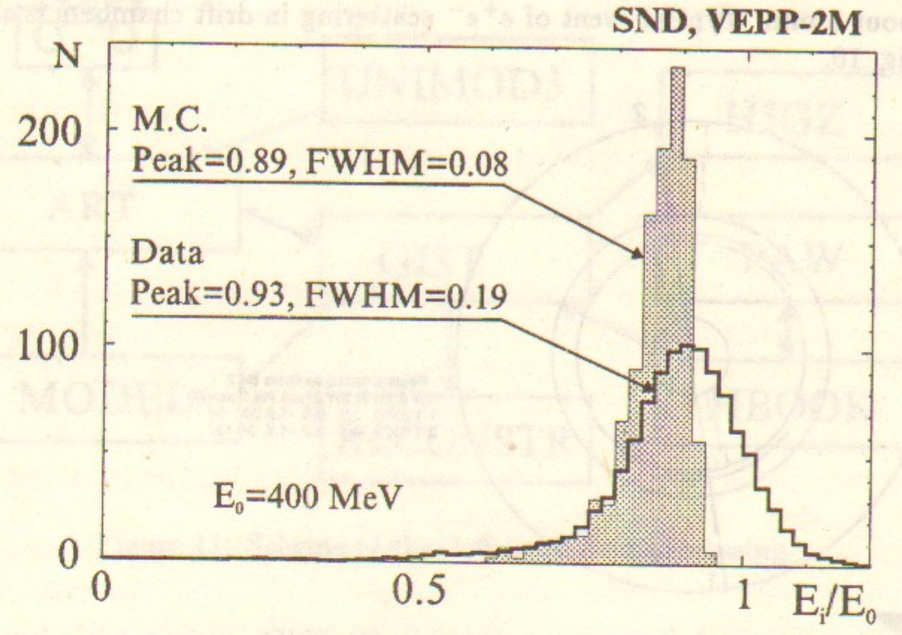

Figure 8: Experimental and simulated energy deposition spectra of 400 MeV electrons

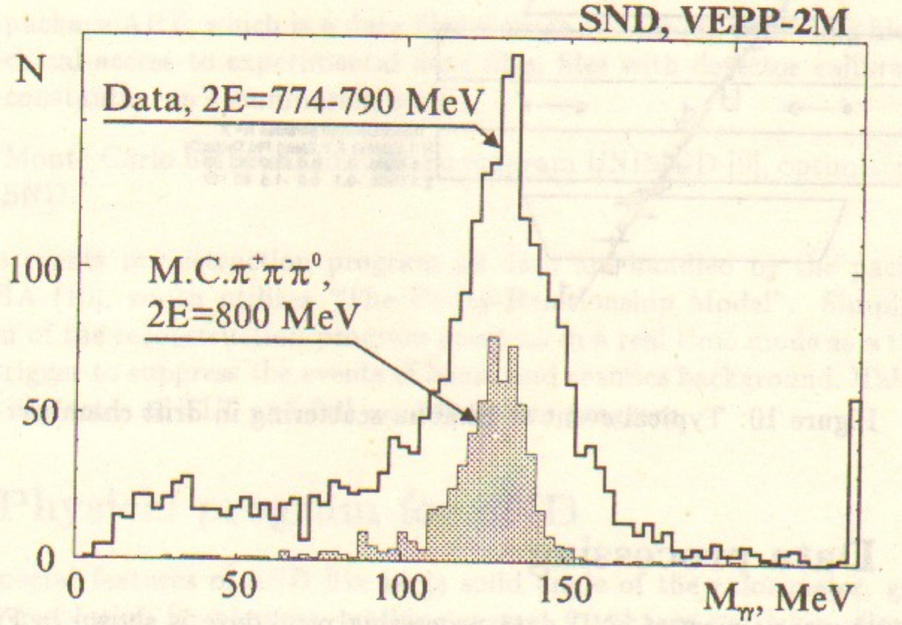

Figure 9: Measured and simulated two-photon invariant mass spectra in the vicinity of ω–meson resonance

is about 3 mm. Typical event of e^+e^- scattering in drift chambers is shown in Fig. 10.

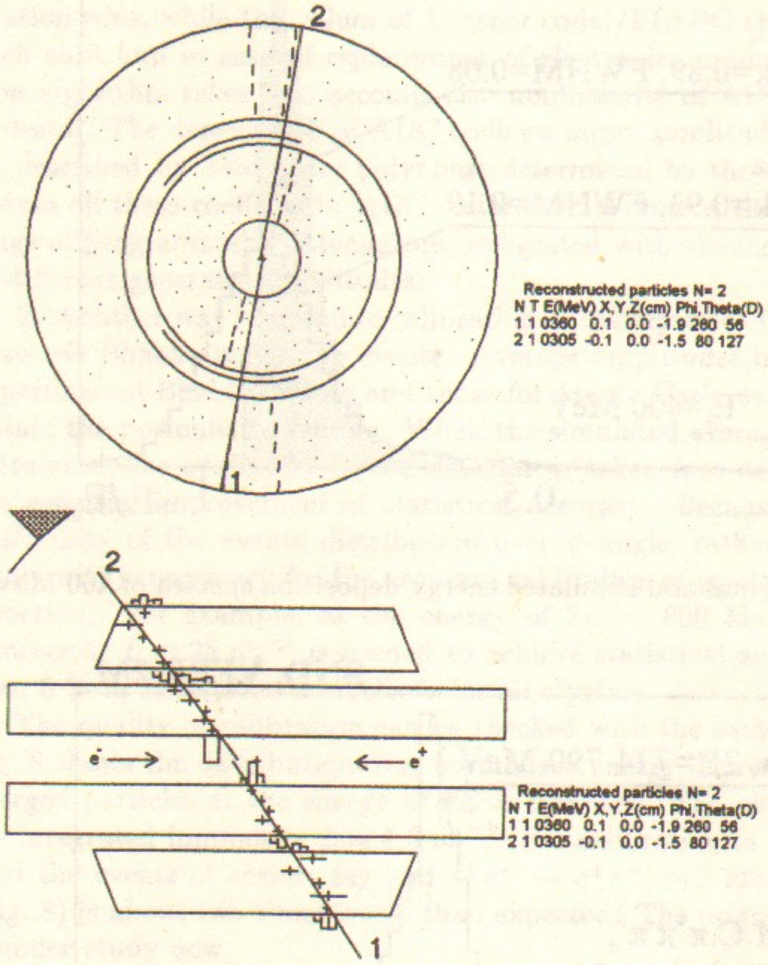

Figure 10: Typical event of Bhabha scattering in drift chambers

6 Data processing

The schematic view of SND data processing procedure is shown in Fig. 11. It is based on the following program packages:

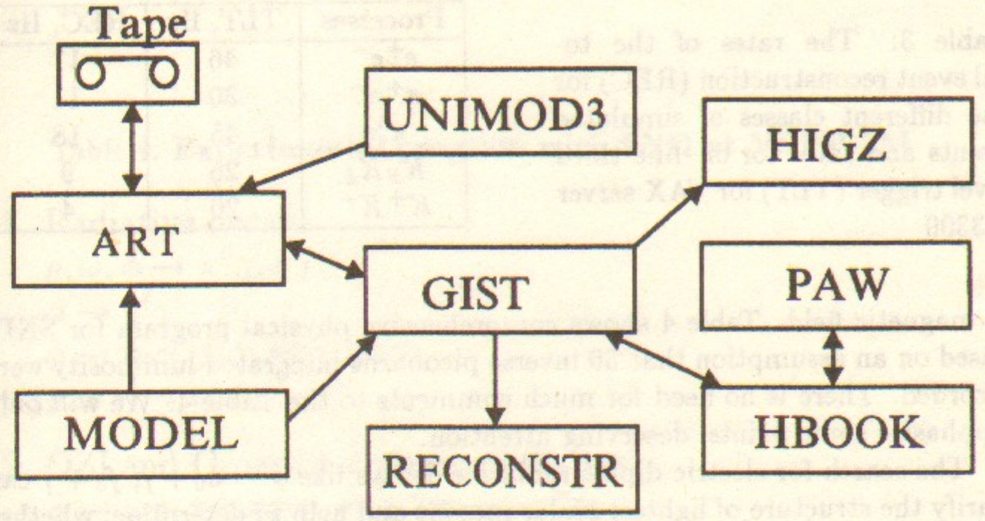

Figure 11: Scheme of the "off-line" data processing

- universal package GIST [7], providing users interface and links with other packages, including ART, PAW, and events visualization programs;
- package ART, which is a data files storage system [8], providing hierarchical access to experimental data files, files with detector calibration constants, run's summaries, etc.;
- Monte Carlo universal simulation program UNIMOD [9], optimized for SND.

In the events reconstruction program all data are handled by the package COCHA [10], which utilizes "The Entity-Relationship Model". Simplified version of the reconstruction program operates in a real time mode as a third level trigger to suppress the events of beam and cosmics background. Table 3 shows the rates of TLT and full reconstruction program.

7 Physical program for SND

The special features of SND like large solid angle of the calorimeter, good energy resolution for photons, tracking system for charge particles, allow to reconstruct all kinematic parameters in events with both charged and neutral particles, allow to study wide range of physical processes, in spite of absense

Table 3: The rates of the total event reconstruction (REC) for the different classes of simulated events and rates for on–line third level trigger (TLT) for VAX server – 3300

Processes	TLT, Hz	REC, Hz
e^+e^-	46	17
$\pi^+\pi^-$	30	11
$\pi^0\gamma$	45	18
K_SK_L	25	9
K^+K^-	20	4

of magnetic field. Table 4 shows comprehensive physical program for SND, based on an assumption that 50 inverse picobarns integrated luminosity were recorded. There is no need for much comments to the Table 4. We will only emphasize some points, deserving attention.

The search for electric dipole radiative decays like $\phi \to a_0 + \gamma$, $f_0 + \gamma$ can clarify the structure of lightest scalar mesons and help to determine, whether or not are they mixed with 4-quark states.

The careful study of e^+e^- annihilation cross section into hadrons is important for precision theoretical calculations of hadron contribution into muon anomalous magnetic moment (AMM) [13]. In the energy range $2E < 1$ GeV, we have to measure the cross section with the uncertainty of 0.5%. The corresponding error in AMM calculations would be 0.2 ppm.

The hadronic cross-section is also of great importance to solve the problem of existence and location of light vector meson radial exitations ρ, ω, ϕ. This cross section also contributes significantly into some decay spectra and branching ratios of τ-lepton, D- and B-mesons.

Higher order QED reactions $2 \to 3, 4, 5$ where all particles are electrons and photons, produced at large angles with respect to the beams, are interesting from the point of view of QED tests. Their cross sections, which are proportional $\sim 1/E^2$, are high enough to study them at low energy e^+e^- machine.

The large number of processes, listed in Table 4, shows wide range of particle research, available at VEPP-2M with SND detector.

Acknowledgements

This work is sponsored in part by the Russian Fund for Fundamental Researches, Grants No. 93–02–15553 and 93–02–03295.

Table 4: **Experimental program with SND at VEPP-2M**

1. Radiative decays
   $\rho, \omega, \phi \to \pi^0\gamma, \eta\gamma$
   $\phi \to \eta'\gamma$
   $\phi \to a_0\gamma, f_0\gamma, \pi\pi\gamma, \eta\pi\gamma$
   $\rho, \omega \to \pi\pi\gamma$
2. OZI and G-parity suppressed decays
   $\phi \to \omega\pi, \pi\pi, \eta\pi\pi$; $\rho \to 3\pi$; $\omega \to 2\pi$
3. Electromagnetic decays
   $\rho, \omega, \phi \to \eta e^+e^-, \pi^0 e^+e^-$
4. e^+e^- annihilation into hadrons
   $e^+e^- \to 2\pi, 3\pi, 4\pi, 5\pi$
   $e^+e^- \to \omega\pi, \eta\pi\pi, \phi\pi$
   $e^+e^- \to K^+K^-, K_SK_L, KK\pi$
5. Test of QED
   $e^+e^- \to 3\gamma, e^+e^-\gamma$ $(2 \to 3)$
   $e^+e^- \to 4\gamma, e^+e^-\gamma\gamma, 4e$ $(2 \to 4)$
   $e^+e^- \to 5\gamma, 3\gamma e^+e^-, 4e\gamma$ $(2 \to 5)$
6. Search for rare K_S decays
   $K_S \to 2\gamma, 3\pi^0, 2\pi^0\gamma, \pi^0\gamma\gamma, \pi^0 e^+e^-$
7. Search for rare η decays
   $\eta \to 3\gamma, e^+e^-, 4e$
8. Search for C-even reactions
   $e^+e^- \to \eta', a_0, f_0, a_2, f_2$

References

[1] *G.M. Tumaikin.* Proceedings of the 10-th International Conference on High Energy Particle Accelerators. Serpukhov, 1977, vol.1, p.443

[2] *V.B.Golubev et al.* Nuclear Instruments and Methods 227(1984)467

[3] *S.I.Dolinsky et al.* Physics Reports, V.202, No.3, (1991), 99

[4] *CMD-2 Collaboration,* ICFA Instrumentation Bulletin, 5, (1988), 18
it R.R.Akhmetshin et al. Preprint BudkerINP 95–35, Novosibirsk, 1995

[5] *V.V.Anashin et al.* in: Proceedings of V-th International Conference on Instrumentation for Colliding Beam Physics, Novosibirsk, March 1990, (World Scientific), p.360;
V.M.Aulchenko et al., in: Proceedings of Workshop on Physics and detectors for DAFNE, Frascati, April 1991, p.605

[6] *M.Oreglia et al.* Physical Review, D25,(1982),2259.

[7] *А.Д. Букин, В.Н. Иванченко.* Гистограммная программа GIST. Препринт ИЯФ 93–81, Новосибирск, 1993.

[8] *А.А. Король.* Архив экспериментальных данных. Препринт ИЯФ 94–62, Новосибирск, 1994.

[9] *A.D. Bukin et al.* UNIMOD2 — Universal Code for Simulation of e^+e^- Colliding Beam Experiments. 5. Version 2.0 User Guide. Preprint BudkerINP 94–20, Novosibirsk, 1994

[10] *В.Н. Иванченко.* СОСНА — пакет программ для структурирования экспериментальных данных. Препринт ИЯФ 94–25, Новосибирск, 1994.

[11] *V.M.Aulchenko et al.* Preprint INP 85–122, Novosibirsk, 1985

[12] *V.M.Aulchenko et al.* Data acquisition system for new detector in INP. Proceedings of the International Conference on Calorimetry in High Energy Physics, FNAL, 29 Oct – 1 Nov, 1990
В.М.Аульченко, С.Е.Бару, Г.А.Савинов. Электроника новых детекторов ИЯФ для экспериментов на встречных пучках. Международный симпозиум по координатным детекторам в физике высоких энергий (1Д1.13–88–172). Изд-во ОИЯИ, Дубна, 1988

[13] (g-2) Design Report, BNL, 1995

Contents

V.M.Aulchenko, M.N.Achasov, T.V.Baier, P.M.Beschastnov,
A.D.Bukin, D.A.Bukin, S.V.Burdin, A.V.Bozhenok, B.O.Baibusinov,
V.V.Danilov, S.I.Dolinsky, V.P.Druzhinin, M.S.Dubrovin,
I.A.Gaponenko, V.B.Golubev, V.N.Ivanchenko, S.V.Koshuba,
A.A.Korol, I.A.Koop, A.P.Lysenko, I.N.Nesterenko, E.V.Pakhtusova,
E.A.Perevedentsev, A.A.Polunin, V.I.Ptitsyn, E.G.Pozdeev,
A.A.Salnikov, S.I.Serednyakov, Yu.M.Shatunov, M.A.Shubin,
V.A.Sidorov, Z.K.Silagadze, A.N.Skrinsky, Yu.V.Usov,
Yu.S.Velikzhanin

Beginning of the Experiments with SND Detector
at e^+e^- Collider VEPP-2M

В.М.Аульченко, М.Н.Ачасов, Т.В.Байер, П.М.Бесчастнов,
А.Д.Букин, Д.А.Букин, С.В.Бурдин, А.В.Боженок, Б.О.Байбусинов,
В.В.Данилов, С.И.Долинский, В.П.Дружинин, М.С.Дубровин,
И.А.Гапоненко, В.Б.Голубев, В.Н.Иванченко, С.В.Кошуба,
А.А.Король, И.А.Кооп, А.П.Лысенко, И.Н.Нестеренко, Е.В.Пахтусова,
Е.А.Переведенцев, А.А.Полунин, В.И.Птицын, Е.Г.Поздеев,
А.А.Сальников, С.И.Середняков, Ю.М.Шатунов, М.А.Шубин,
В.А.Сидоров, З.К.Силагадзе, А.Н.Скринский, Ю.В.Усов,
Ю.С.Великжанин

Начало экспериментов с детектором СНД
на e^+e^- накопителе VEPP-2M

Budker INP 95–56

Ответственный за выпуск С.Г.Попов
Работа поступила 5 июля 1995 г.

Сдано в набор 6 июля 1995 г.
Подписано в печать 6 июля 1995 г.
Формат бумаги 60×90 1/16 Объем 1,0 печ.л., 0,9 уч.-изд.л.
Тираж 250 экз. Бесплатно. Заказ №56

Обработано на IBM PC и отпечатано на
ротапринте ГНЦ РФ "ИЯФ им. Г.И.Будкера СО РАН",
Новосибирск, 630090, пр. академика Лаврентьева, 11.